

# Design of Adaptive Sliding Mode Controller for Robust Yaw Stabilization of In-wheel-motor-driven Electric Vehicles

Kanghyun Nam<sup>1</sup>, Sehoon Oh<sup>1</sup>, Hiroshi Fujimoto<sup>2</sup>, and Yoichi Hori<sup>2</sup>

<sup>1</sup>*Department of Electrical Engineering, Hongo Bunkyo-ku Tokyo 113-8656,*  
nam@hori.k.u-tokyo.ac.jp; sehoon@hori.k.u-tokyo.ac.jp

<sup>2</sup>*Department of Advanced Energy, Kashiwa, Chiba, Japan 277-8561,*  
fujimoto@k.u-tokyo.ac.jp; hori@k.u-tokyo.ac.jp

---

## Abstract

A robust yaw stability control system is designed to stabilize the vehicle yaw motion. Since the vehicles undergo changes in parameters and disturbances with respect to the wide range of driving condition, e.g., tire-road conditions, a robust control design technique is required to guarantee system stability. In this paper, a sliding mode control methodology is applied to make vehicle yaw rate to track its reference with robustness against model uncertainties and disturbances. A parameter adaptation law is applied to estimate varying vehicle parameters with respect to road conditions and is incorporated into sliding mode control framework. The control performance of the proposed control system is evaluated through computer simulation using CarSim vehicle model which proved to give a good description of the dynamics of an experimental in-wheel-motor-driven electric vehicle. Moreover, field tests were carried out to verify the effectiveness of the proposed adaptive sliding mode controller.

*Keywords: Adaptive sliding mode control, In-wheel motor-driven electric vehicle, Yaw stabilization*

---

## 1 Introduction

Due to the increasing concerns about advanced motion control of electric vehicles with in-wheel motors, a great deal of research on dynamics control for electric vehicles has been carried out [1]–[5]. Advanced motion control systems for electric vehicles, slip prevention, spinout prevention, and excessive roll prevention, are referred to as yaw stability control and roll stability control, respectively. Compared with internal combustion engine vehicles, electric vehicles with in-wheel motors have several advantages in the viewpoint of motion control [1], [3].

1. The torque generation of driving motors is very fast and accurate.
2. The driving torque can be easily measured from motor current.
3. Each wheel with an in-wheel motor can be independently controlled.

The purpose of vehicle motion controls is to prevent unintended vehicle behavior through active vehicle control and assist drivers in maintaining controllability and stability of vehicles. The main goal of most motion control systems is to control the yaw rate of the vehicles. In [6], direct yaw moment control based on side slip angle estimation was proposed for improving the stability of in-wheel-motor-driven electric vehicles (IWM-EV). A fuzzy-rule-based control and sliding mode control algorithms for vehicle stability enhancement were proposed and evaluated through experiments [7], [8]. A novel yaw stability control method based on robust yaw moment observer (YMO) design is presented and its practical effectiveness was verified through various field tests [9]. Parameter uncertainties shown in a vehicle model and external disturbances acting on vehicles are compensated by the disturbance observer and yaw stabilization is realized through yaw rate feedback control. In this paper, a sliding model control method with pa-

parameter adaptation is employed for robust yaw stabilization of electric vehicles. The proposed control structure employs a reference generator, which is designed from driver's commands, a sliding mode controller, and parameter adaptation laws. The sliding mode control technique is well-known robust control methodology particularly suitable for dealing with nonlinear systems with model uncertainties and disturbances like the considered vehicle systems. Since the vehicles operate under wide range of road conditions and speed, the controller should provide robustness against varying parameters and undesired disturbances all over the driving regions. In [10], a cascade vehicle yaw stability control system was designed with the sliding mode and backstepping control approaches. In [11], a vehicle yaw controller via second-order sliding mode technique was designed to guarantee robust stability in front of disturbances and model uncertainties.

In order to compensate the disturbances and model uncertainties existing in control law, the adaptive sliding mode control method is applied. By combining with the defined sliding surface, a sliding mode controller is re-designed such that the state (i.e., yaw rate) is moved from the outside to inside of the region, and finally, it remains inside the region even though there are model uncertainties and disturbances, which can be estimated and then rejected by adaptation law.

In order to verify the control performances, the computer simulation is performed using a CarSim vehicle model, which proved to give a good description of the dynamics of an in-wheel-motor driven electric vehicle developed by the Hori/Fujimoto research team (see [12] and [13]), as compared with test data. This paper is organized as follows. A vehicle model for control design is introduced in Section 2. A sliding mode controller combining parameter adaptation approaches is proposed and the stability of both a sliding mode control law and an adaptation law is proved in Section 3. The simulation and experiment results are presented and discussed in Section 4. Finally, conclusions and future works are presented in Section 5.

## 2 Vehicle Modeling

In this section, a yaw plane model is introduced to describe the motion of an in-wheel-motor driven electric vehicle. The main difference with commonly used vehicle dynamics is that the direct yaw moment is an additional input variable, which is generated by motor torque difference between each wheel. The yaw plane representation with direct yaw moment is shown in Fig. 1.

From the linear single track vehicle model as shown in Fig. 1 (b), the governing equation for yaw motion is given by

$$I_z \dot{\gamma} = l_f F_f^y \cos \delta_f - l_r F_r^y + M_z \quad (1)$$

where  $\gamma$  is the yaw rate,  $I_z$  is the yaw moment of inertia,  $F_f^y$  and  $F_r^y$  are the front and rear lat-

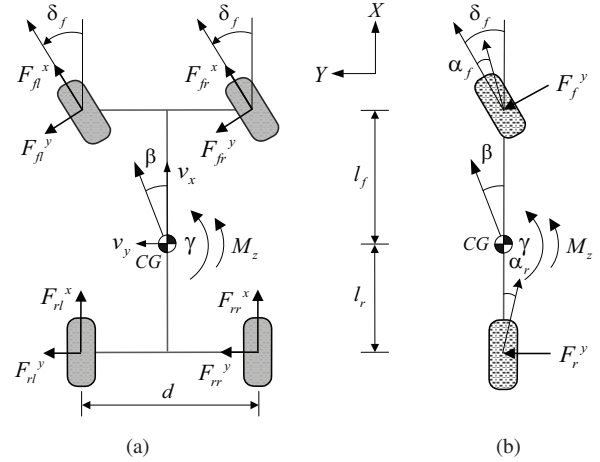


Figure 1: Planar vehicle model: (a) Four wheel model, (b) Single track model (i.e., bicycle model).

eral tire forces, respectively,  $l_f$  and  $l_r$  are the distance from vehicle center of gravity (CG) to front and rear axles,  $\delta_f$  is the front steering angle, and the yaw moment  $M_z$  indicates a direct yaw moment control input, which is generated by the independent torque control of in-wheel motors and is used to stabilize the vehicle motion, and can be calculated as follows:

$$M_z = \frac{d}{2}(F_{rr}^x - F_{rl}^x) + \frac{d}{2}(F_{fr}^x - F_{fl}^x) \cos \delta_f \quad (2)$$

Here, longitudinal tire forces can be obtained from a driving force observer (shown in Fig. 2), which is designed based on wheel rotational motion [14], and the estimate of longitudinal tire force is expressed as

$$\hat{F}_i^x = \frac{\omega_D}{s + \omega_D} \left( \frac{T_i^m - I_\omega \omega_i s}{r} \right) \quad (3)$$

where  $\hat{F}_i^x$  is the estimated longitudinal tire force at  $i$ th wheel,  $T_i^m$  is the motor torque acting on each wheel,  $I_\omega$  is the wheel inertia,  $\omega_i$  is an angular velocity of the wheel,  $r$  is an effective tire radius, and  $\omega_D$  is a cutoff frequency of the applied low-pass filter which rejects high frequency noises cause by time derivative of  $\omega_i$ .

In order to describe the vehicle motion, a linear tire model is used. For small tire slip angles, the lateral tire forces can be linearly approximated as follows:

$$F_f^y = -2C_f \alpha_f = -2C_f \left( \beta + \frac{\gamma l_f}{v_x} - \delta_f \right) \quad (4)$$

$$F_r^y = -2C_r \alpha_r = -2C_r \left( \beta - \frac{\gamma l_r}{v_x} \right) \quad (5)$$

where  $\beta$  is a vehicle sideslip angle,  $v_x$  is the vehicle speed,  $\alpha_f$  and  $\alpha_r$  are tire slip angles of front

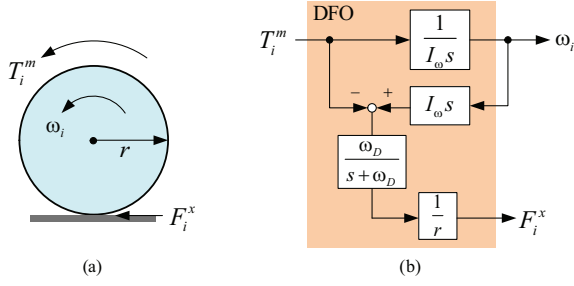


Figure 2: (a) Wheel rotational motion, (b) Block diagram of a driving force observer (DFO) [14].

and rear tires, and  $C_f$  and  $C_r$  are the front and rear tire cornering stiffness, respectively. From (1), (4), and (5), yaw dynamics is expressed as

$$I_z \dot{\gamma} = -\frac{2(l_f^2 C_f + l_r^2 C_r)}{v_x} \gamma + 2l_f C_f \delta_f + M_z - 2\beta(l_f C_f - l_r C_r) + M_d \quad (6)$$

where  $M_d$  is the yaw moment disturbance which may be caused by unstable road condition or side wind etc., the yaw moment generated by vehicle sideslip, i.e.,  $-2\beta(l_f C_f - l_r C_r)$ , is considered as a disturbance. In  $\bar{M}_d$  is defined as a lumped yaw moment disturbance and can be expressed as

$$\bar{M}_d = -2\beta(l_f C_f - l_r C_r) + M_d \quad (7)$$

*Assumption:* The lumped disturbance  $\bar{M}_d(t)$ , which varies with tire-road condition and vehicle parameters, is bounded and satisfy the following condition

$$\|\bar{M}_d(t)\| \leq \kappa \quad (8)$$

where  $\kappa$  is the upper bound of the disturbance. Thus, yaw dynamics equation (6) can be considered as a time-varying two input and one output system and rewritten as

$$I_z \dot{\gamma} = -B\gamma + 2l_f C_f \delta_f + M_z + \bar{M}_d \quad (9)$$

where  $B$  is defined as a yaw damping coefficient which varies with vehicle speed and tire-road condition.

## 3 Design of Adaptive Sliding Mode Controller

### 3.1 Overall Control structure

The proposed control system is depicted in Fig. 3. A reference generator makes a desired yaw rate  $\gamma_d$  from driver's steering command  $\delta_{cmd}$  and

vehicle speed  $v_x$ . The feedback controller is designed to make yaw moment to compensate yaw rate tracking error (i.e.,  $\gamma_d - \gamma$ ) based on the standard sliding mode control methodology. For treating model uncertainties and disturbances existing in a feedback control law, parameters in a designed sliding mode control law are updated according to adaptation laws. The external input  $M_d$  accounts for yaw moment disturbance caused by lateral wind, unbalanced road conditions, and unbalanced tire pressure, etc. With well-tuned control parameters, a proposed controller contributes to keeping the vehicle yaw rate following its target commanded by the driver.

### 3.2 Reference Generation: Desired Yaw Response

The objective of the yaw stability control is to improve the vehicle steadiness and transient response properties, enhancing vehicle handling performance and maintaining stability in those cornering maneuvers, i.e., the yaw rate  $\gamma$  should be close to desired vehicle responses (i.e.,  $\gamma_d$ ). The desired vehicle response is defined based on driver's cornering intention (e.g., driver's steering command and vehicle speed). Desired vehicle yaw rate response for given steering angle and vehicle speed is obtained as follows:

$$\begin{aligned} \gamma_d &= \frac{K(v_x)}{1 + \tau s} \cdot \delta_{cmd} \\ K(v_x) &= \frac{1}{1 + k_{us} v_x^2} \frac{v_x}{l}, \\ k_{us} &= \frac{m(l_r C_r - l_f C_f)}{2l^2 C_f C_r} \end{aligned} \quad (10)$$

where  $\tau$  is a cutoff frequency of desired model filters,  $k_{us}$  is a vehicle stability factor which explains the steering characteristics of the vehicles. The sign of  $l_r C_r - l_f C_f$  in  $k_{us}$  represents the vehicle motion behavior by steering action and the steering characteristics are classified as follows:

$$\begin{aligned} l_r C_r - l_f C_f &> 0 & : \text{under steering} \\ l_r C_r - l_f C_f &= 0 & : \text{neutral steering} \\ l_r C_r - l_f C_f &< 0 & : \text{over steering.} \end{aligned} \quad (11)$$

### 3.3 Sliding Mode Control

It is well known that sliding mode control is a robust control method to stabilize nonlinear and uncertain systems which have attractive features to keep the systems insensitive to the uncertainties on the sliding surface [15]. The conventional sliding mode control design approach consists of two steps. First, a sliding surface is designed such that the system trajectory along the surface acquires certain desired properties. Then, a discontinuous control is designed such that the system trajectories reach the sliding surface in finite time. A sliding mode control as a general design

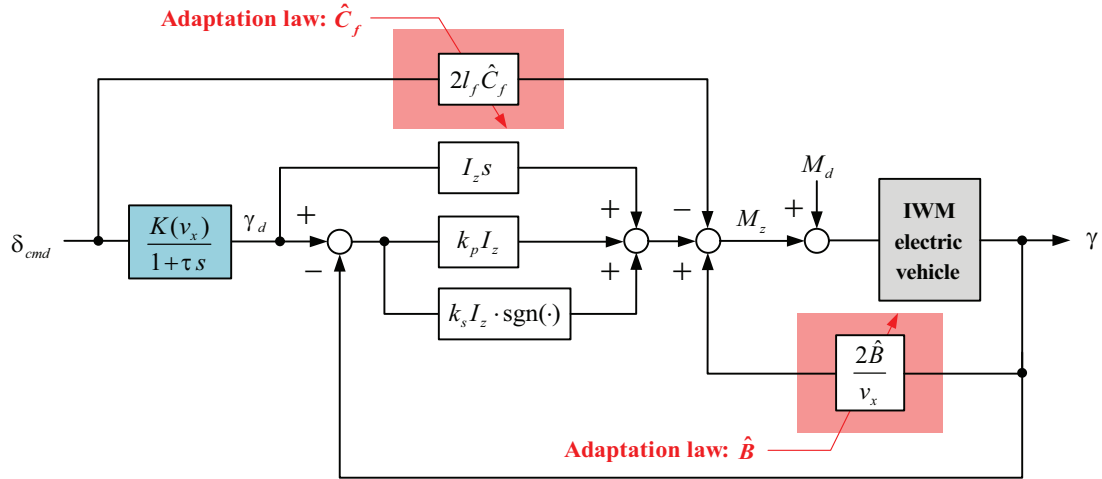


Figure 3: Block diagram of an adaptive sliding mode controller.

technique for control systems has been well established, the advantages of a sliding model control method are:

- fast response and good transient performance
- its robustness against a large class of perturbations or model uncertainties
- the possibility of stabilizing some complex nonlinear systems which are difficult to stabilize by continuous state feedback laws.

Based on above advantages, sliding mode control has been applied to vehicle control systems [10] and [11]. As usual in the sliding mode control technique, the control forces the system evolution on a certain surface which guarantees the achievement of the control requirements. In order to achieve control objective, i.e.,  $\lim_{t \rightarrow \infty} S(t) = 0$ , the sliding surface  $S(t)$  is defined as

$$S = \gamma - \gamma_d \quad (12)$$

Here we can see that the sliding condition  $S(t) = 0$  means a zero tracking error.

By designing a satisfactory dynamics feedback control law, the trajectory of the closed-loop system can be driven on the sliding surface (12) and evolve along it, and yaw stabilization can be achieved. In order to achieve control requirements, a following reaching condition to be satisfied is designed as

$$\dot{S} = -k_P S - k_S \cdot \text{sgn}(S) \quad (13)$$

where the  $k_P > 0$  is a control parameter which determines the convergence rate of a tracking error, the  $k_S > 0$  is a control parameter which should be tuned according to bound of uncertainties and disturbances.

From (6), (12), and (13), we can apply standard sliding mode control method [15] and thereby the following control law can be obtained

$$M_z(t) = I_z \dot{\gamma}_d(t) + \frac{2B}{v_x(t)} \gamma(t) - 2l_f C_f \delta_f(t) - k_P I_z S - k_S I_z \cdot \text{sgn}(S) \quad (14)$$

We can prove that the sliding mode control law (14) makes the closed-loop control system asymptotically stable by introducing following positive definite Lyapunov function

$$V = \frac{1}{2} S^2 \quad (15)$$

The time derivative of (15) is

$$\begin{aligned} \dot{V} &= S \dot{S} = S(\dot{\gamma} - \dot{\gamma}_d) \\ &= S \left[ -\frac{2(l_f^2 C_f + l_r^2 C_r)}{I_z v_x} \gamma + \frac{2l_f C_f \delta_f}{I_z} + \frac{M_z}{I_z} - \dot{\gamma}_d \right] \\ &= S(-k_P S - k_S \cdot \text{sgn}(S)) \\ &= -k_P S^2 - k_S |S| < 0. \end{aligned} \quad (16)$$

Thus, the control objective, i.e.,  $S(t) \rightarrow 0$  as  $t \rightarrow \infty$ , can be achieved by the control law (14).

*Remark 1:* In (14), the sliding mode switching gain  $k_S$  is selected considering uncertainty and disturbance bound. From assumption (8),  $k_S$  should be determined by considering the disturbance bound. Moreover, the maximum  $k_S$  which can be selected is limited by the maximum torque that an in-wheel motor generates. By properly tuning  $k_P$  and  $k_S$ , the chattering in control law is also reduced.

### 3.4 Sliding Mode Control with Parameter Adaptation

For treating the disturbance and inertia uncertainty existing in the control law (14), adaptive control method is a natural choice and has been widely applied. Combing with the defined sliding surface, a sliding mode controller can be designed such that the system state is moved from the outside to the inside of the region, and finally remains inside the region in spite of the uncertainty and disturbance which can be estimated and then rejected under the help of adaptive law. Thus, based on above analysis, the control law (14) is modified as

$$M_z(t) = I_z \dot{\gamma}_d(t) + \frac{2\hat{B}}{v_x(t)} \gamma(t) - 2l_f \hat{C}_f \delta_f(t) - k_P I_z S - k_S I_z \cdot \text{sgn}(S) \quad (17)$$

where the adaptation law for the estimated parameter  $\hat{B}$  and  $\hat{C}_f$  are chosen as

$$\dot{\hat{B}}(t) = -\frac{2k_1}{I_z v_x(t)} \gamma(t) S - \eta_1 k_1 \tilde{B} \quad (18)$$

$$\dot{\hat{C}}_f(t) = -\frac{2l_f k_2}{I_z} \delta_f(t) S - \eta_2 k_2 \tilde{C}_f. \quad (19)$$

Here  $\tilde{B} = \hat{B}(t) - B$ ,  $\tilde{C}_f = \hat{C}_f(t) - C_f$ ,  $k_1$  and  $k_2$  are adaptation gains which determine the update rate,  $\eta_1$  and  $\eta_2$  are positive constant values.

*Remark 2:* The main objective of parameter adaptation is to compensate parameter uncertainty and disturbance which varies with tire-road conditions. The adaptation law (18), (19) consists of a tracking error (i.e.,  $S(t)$ ) correction term. An adaptation law is rewritten in terms of Laplace transform as follows:

$$\hat{B}(s) = \frac{\eta_1 k_1}{s + \eta_1 k_1} B + \left( \frac{2k_1}{I_z v_x} \right) \frac{1}{s + \eta_1 k_1} \gamma S \quad (20)$$

$$\hat{C}_f(s) = \frac{\eta_2 k_2}{s + \eta_2 k_2} C_f + \left( \frac{2k_2 l_f}{I_z} \right) \frac{1}{s + \eta_2 k_2} \delta_f S \quad (21)$$

where the small  $s$  is a Laplace variable.

**Theorem.** Considering vehicle yaw dynamics with designed sliding surface, the trajectory of the closed-loop control system can be driven on to the sliding surface  $S(t) = 0$  with the proposed adaptive control law and adaptation update law, and finally converge to the pre-defined reference trajectory.

**Proof:** Consider the following positive definite Lyapunov function:

$$V = \frac{1}{2} S^2 + \frac{1}{2k_1} \tilde{B}^2 + \frac{1}{2k_2} \tilde{C}_f^2. \quad (22)$$

The time derivative of (22) is as follows:

$$\begin{aligned} \dot{V} &= S \dot{S} + \frac{1}{k_1} \tilde{B} \dot{\tilde{B}} + \frac{1}{k_2} \tilde{C}_f \dot{\tilde{C}}_f \\ &= S \left[ \frac{2\gamma}{I_z v_x} \tilde{B} - \frac{2l_f \delta_f}{I_z} \tilde{C}_f - k_P S \right. \\ &\quad \left. - k_S \cdot \text{sgn}(S) \right] + \frac{1}{k_1} \tilde{B} \dot{\tilde{B}} + \frac{1}{k_2} \tilde{C}_f \dot{\tilde{C}}_f. \end{aligned} \quad (23)$$

With the adaptation law, this can be rewritten as follows:

$$\begin{aligned} \dot{V} &= S \dot{S} + \frac{1}{k_1} \tilde{B} \dot{\tilde{B}} + \frac{1}{k_2} \tilde{C}_f \dot{\tilde{C}}_f \\ &= S \left[ \frac{2\gamma}{I_z v_x} \tilde{B} - \frac{2l_f \delta_f}{I_z} \tilde{C}_f - k_P S \right. \\ &\quad \left. - k_S \cdot \text{sgn}(S) \right] \\ &\quad + \frac{1}{k_1} \tilde{B} \left( -\frac{2k_1}{I_z v_x} \gamma S - \eta_1 k_1 \tilde{B} \right) \\ &\quad + \frac{1}{k_2} \tilde{C}_f \left( -\frac{2l_f k_2}{I_z} \delta_f(t) S - \eta_2 k_2 \tilde{C}_f \right) \\ &= -k_P S^2 - k_S |S| - \eta_1 \tilde{B}^2 - \eta_2 \tilde{C}_f^2 < 0. \end{aligned} \quad (24)$$

This shows that the tracking error  $S(t)$  asymptotically converges to zero and the yaw stabilization is achieved.

*Remark 3:* The control parameters  $k_P$  and  $k_S$  in control law (14) play a important role in control system. These parameters determine the convergence rate of the sliding surface. It is noted that a larger  $k_P$  will force the yaw rate to converge to the desired yaw rate trajectory with a high speed. However, in practice, a compromise between the response speed and control input should be made. Since a too big  $k_P$  will require a very high control input, which is always bounded in reality. Therefore, the control parameter  $k_P$  can not be selected too large.

*Remark 4:* The control law (14) is discontinuous when crossing the sliding surface  $S(t) = 0$ , which may lead to the undesirable chattering problem due to the measurement noise and some actuator delay. This problem can be eliminated by replacing a discontinuous switching function (i.e.,  $\text{sgn}(S)$ ) with a saturation function  $\text{sat}(S)$  with the boundary layer thickness  $\Phi$  as the continuous approximation of a signum function

$$\begin{aligned} \text{sgn}(S) &\approx \text{sat} \left( \frac{S}{\Phi} \right) \\ &= \begin{cases} \frac{S}{\Phi}, & \text{if } \left| \frac{S}{\Phi} \right| < 1 \\ \text{sgn} \left( \frac{S}{\Phi} \right), & \text{otherwise} \end{cases} \end{aligned} \quad (25)$$

Thus, this offers a continuous approximation to the discontinuous sliding mode control law inside the boundary layer and guarantees the motion within the neighborhood of the sliding surface.

### 3.5 In-wheel-motor Torque Distribution

The control yaw moment  $M_z$  is distributed to two rear in-wheel motors based on following equations [9].

$$M_z = \frac{d}{2}(F_{rr}^x - F_{rl}^x) \quad (26)$$

$$T_{cmd} = T_{rr}^m + T_{rl}^m \quad (27)$$

where it is assumed that the vehicle is rear wheel driving, the torque control commands to two rear in-wheel motors are calculated as  $T_{rr}^m = rF_{rr}^x$  and  $T_{rl}^m = rF_{rl}^x$ , respectively.

## 4 Simulation and Experiment

### 4.1 Simulation Study

Computer simulations were performed to evaluate the proposed control system. Based on specifications of an experimental electric vehicle, the simulation vehicle model was obtained using CarSim. Simulation environment using CarSim model and Matlab/simulink were constructed for implementation of proposed control algorithms. The proposed stability control system was evaluated through cosimulation for double lane change and step steering tests. A double lane change test was performed at  $v_x=60$  km/h on a high- $\mu$  road (i.e.,  $\mu=0.9$ ). Fig. 4 shows the simulation results. Fig. 4(a) and (b) represent updated parameters by defined adaptation laws. It can be seen that parameters (i.e.,  $B$  and  $C_f$ ) stay close to nominal values when the sliding surface is almost the same as zero, on the other hand, parameters are adapted when the tracking error exists. Fig. 4 (c),(d) indicates the control law  $M_z$  and control torque command of in-wheel motors, respectively. From Fig. 4 (e) and (f), we can see that the vehicle with a proposed controller well tracks the desired vehicle response with a small tracking error.

Fig. 5 shows the results of a step steering test. In order to verify the robustness of a proposed controller, the external yaw moment disturbance ( $M_d = 300$  Nm) is intentionally inserted at time instant  $t = 12$  sec.

As can be seen from Fig. 5(e), if the control is set off, the vehicle shows the spin-out, which causes the vehicles to lose stability and unable to accomplish the desired vehicle motion. From simulation results Fig. 4(c) and Fig. 5(c), we can see that the control law could avoid undesirable chattering through the continuous approximation of a signum function.

### 4.2 Experimental Verification

The proposed adaptive sliding mode controller was implemented on the experimental in-wheel-motor-driven electric vehicle shown in Fig. 6. An experimental electric vehicle which was developed by the Hori/Fujimoto research team is equipped with direct-drive motors in each wheel. Fig.7 illustrates the driving motor installed in each wheel. The specification of an experimental electric vehicle used in field tests is presented in Table I.



Figure 6: Experimental in-wheel-motor-driven electric vehicle.

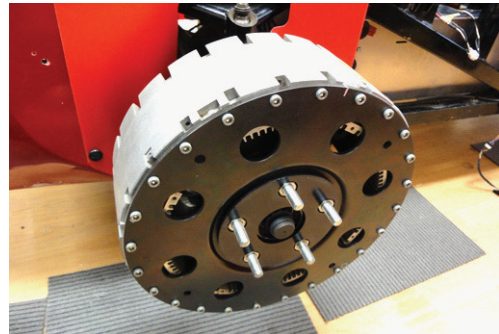


Figure 7: In-wheel motor.

Table 1: Specification of an experimental electric vehicle

Total weight	875 kg
Wheel base	1.715 m
Track width	1.3 m
Yaw moment of inertia	617 kg·m <sup>2</sup>
Spin inertia for each wheel	1.26 kg·m <sup>2</sup>
In-wheel motor	PMSM (outer rotor type)
Max. Power	20.0 kW (for one front motor)
Max. Torque	500 Nm (for one front motor)
Max. Speed	1113 rpm
Controller	AutoBox-DS1103
Steering system	Steer-by-Wire
Suspension system	Double wishbone type
Battery	Lithium-ion

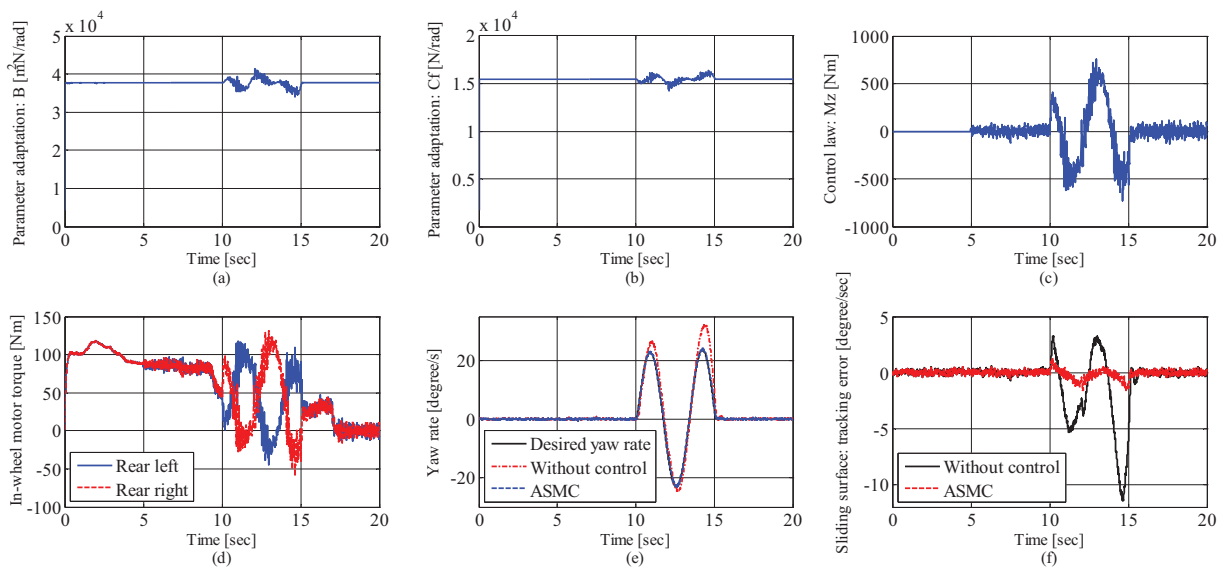


Figure 4: Simulation result of a sine steering test on high- $\mu$ : (a) Estimated parameter:  $\hat{B}$ , (b) Estimated parameter:  $\hat{C}_f$ , (c) Control law:  $M_z$ , (d) Control torque of In-wheel motor, (e) Yaw rate, (f) Sliding surface: tracking error.

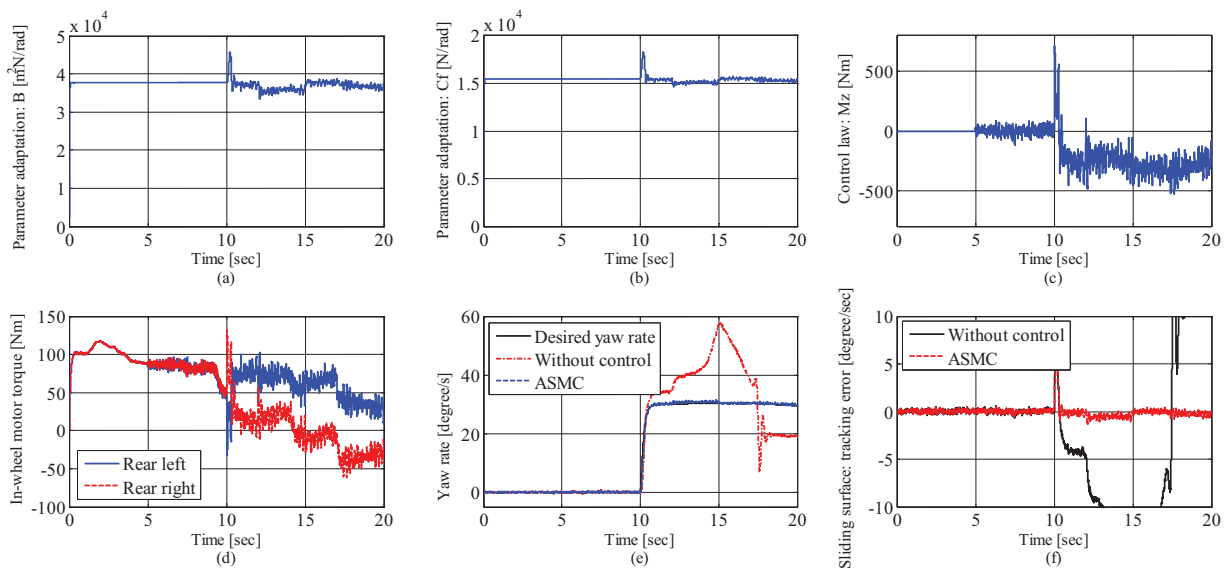


Figure 5: Simulation result of a step steering test on high- $\mu$ : (a) Estimated parameter:  $\hat{B}$ , (b) Estimated parameter:  $\hat{C}_f$ , (c) Control law:  $M_z$ , (d) Control torque of In-wheel motor, (e) Yaw rate, (f) Sliding surface: tracking error.

To demonstrate the performance and effectiveness of the proposed adaptive sliding mode controller, field tests were carried out with following driving conditions; 1) constant vehicle speed, i.e.,  $v_x=20$  km/h; 2) step steering command, i.e.,  $\delta_{cmd}=0.2$  rad; 3) a proposed controller begins to work by enabling the manual control switch; 4) front-wheel driving mode; 5) dry asphalt.

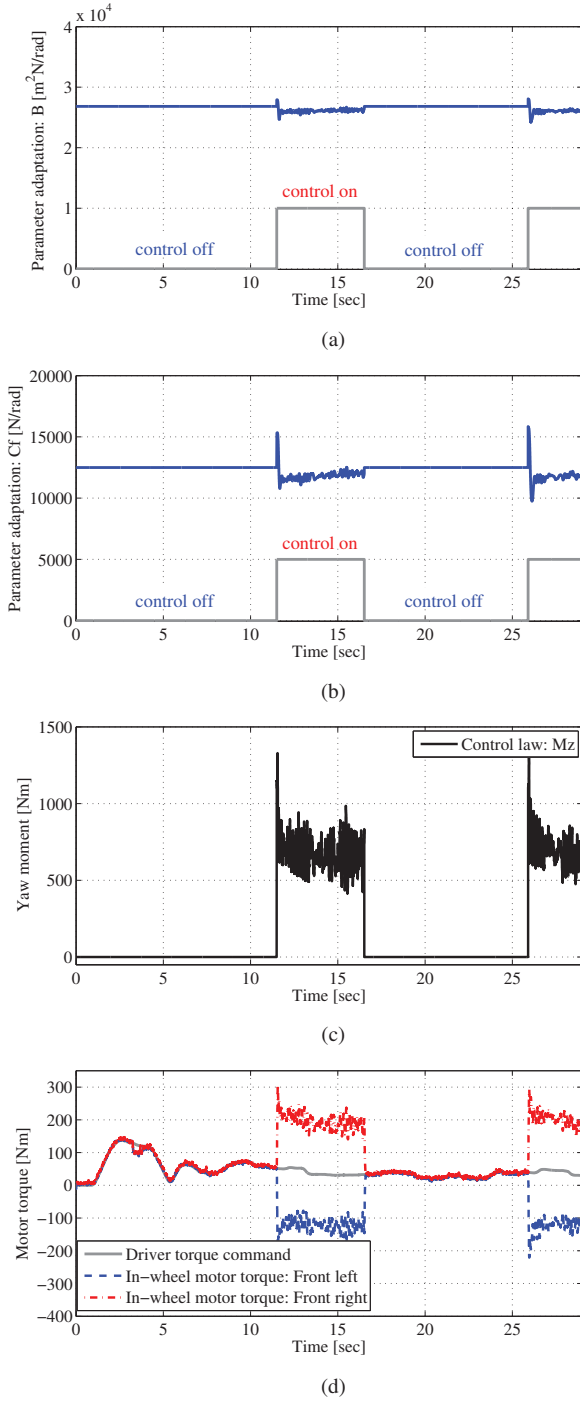


Figure 8: Experimental results of a step steering test at  $v_x=20$  km/h on dry asphalt: (a) Estimated parameter:  $\hat{B}$ . (b) Estimated parameter:  $\hat{C}_f$ . (c) Control law:  $M_z$ . (d) Control torque of In-wheel motor.

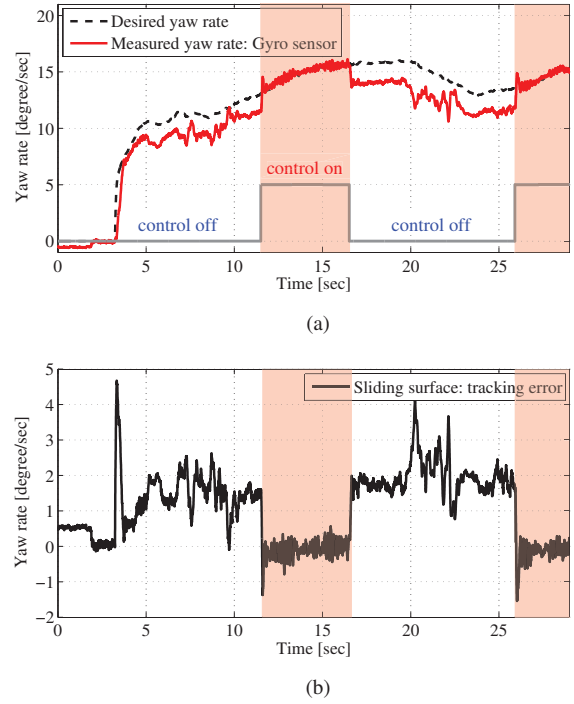


Figure 9: Experimental results of a step steering test at  $v_x=20$  km/h on dry asphalt: (a) Yaw rate. (b) Sliding surface: tracking error.

Fig. 8 shows the experimental results for the proposed adaptive sliding mode controller. A controller begins to work when the control switch (see the thick gray line in Fig. 8 (a),(b)) is turned on by a driver. That is, at  $t=11.5$  sec, a proposed controller begins to work. A step steering input has been commanded by a driver at  $t=5$  sec and an steering motor controller has worked for tracking the driver's steering command. Fig. 8 (a) and (b) represent the results of estimated parameters which are defined in section 3.4. Fig. 8 (c) shows the control law  $M_z$  which is the output of an adaptive sliding mode controller. This control law is allocated to front left and right motors based on (2). In this field tests, front driving motors are used for yaw moment control and following equation is used for control torque distribution.

$$M_z = \frac{d}{2}(F_{fr}^x - F_{fl}^x) \cos \delta_f \quad (28)$$

Measured torques of front left and right in-wheel motors are illustrated in Fig. 8 (d). Fig. 9 represents the results for yaw rate control. We can confirm that the proposed adaptive sliding mode controller stabilizes the vehicle motion from the result of Fig. 9 (a). At  $t=11.5$  sec, the controller begun to work and an actual vehicle yaw rate well tracks the desired yaw rate without a noticeable tracking error. Even though field tests are performed at low speed, the effectiveness of the proposed adaptive sliding mode controller is verified through experimental results of



Fig. 9. The sliding surface  $S(t)$ , which indicates a tracking error of the yaw rate, has converged to zero as shown in Fig. 9. Through theoretical and experimental verification, it is confirmed that tracking performances and stability of the proposed adaptive sliding mode controller are achieved.

## 5 Conclusion and Future Works

This paper has presented an adaptive sliding mode control method for yaw stability enhancement of in-wheel-motor-driven electric vehicles. The proposed control structure is composed of a reference generator, a feedback controller (i.e., sliding mode controller), and parameter adaptation laws. The sliding mode control method, that is capable of guaranteeing robust stability in the presence of model uncertainties and disturbances, is used to stabilize the vehicle yaw motion. The proposed controller has been verified through computer simulation using CarSim. The obtained results show the effectiveness of the proposed control scheme. Moreover, field tests using an experimental electric vehicle are carried out and its effectiveness is verified. In future works, optimal motor torque distribution methods are presented and incorporated into the proposed adaptive sliding mode controller.

## Acknowledgments

This work was supported in part by the Industrial Technology Research Grant Program from New Energy and Industrial Technology Development Organization (NEDO) of Japan.

## References

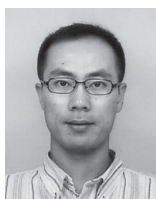
- [1] Y. Hori, *Future vehicle driven by electricity and control-research on four-wheel-motored "UOT Electric March II"*, IEEE Trans. Ind. Electron., vol. 51, no. 5(2004), 654–962.
- [2] G. A. Magallan et.al., *Maximization of the traction forces in a 2WD electric vehicle*, IEEE Trans. Veh. Technol., vol. 60, no. 2(2011), 369–380.
- [3] D. Yin et.al., *A novel traction control for EV based on maximum transmissible torque estimation*, IEEE Trans. Ind. Electron., vol. 56, no. 6(2009), 2086–2094.
- [4] N. Mutoh et.al., *Dynamics of front-and-rear-wheel-independent-drive-type electric vehicles at the time of failure,* IEEE Trans. Ind. Electron., vol. 59, no. 3(2012), 1488–1499.
- [5] R. Wang et.al., *Fault-tolerant control with active fault diagnosis for four-wheel independently-driven electric ground vehicles*, IEEE Trans. Veh. Technol., Vol. 60, No. 9(2011), 4276–4287.
- [6] G. Cong et.al., *Direct yaw-moment control of an in-wheel-motored electric vehicle based on body slip angle fuzzy observer*, IEEE Trans. Ind. Electron., vol. 56, no. 5(2009), 1411–1419.
- [7] K. Kim et.al., *Vehicle stability enhancement of four-wheel-drive hybrid electric vehicle using rear motor control*, IEEE Trans. Veh. Technol., vol. 57, no. 2(2008), 727–735.
- [8] J. Kim et.al., *Control algorithm for an independent motor-drive vehicle*, IEEE Trans. Veh. Technol., vol. 59, no. 7(2010), 3213–3222.
- [9] H. Fujimoto et.al., *Direct yaw-moment control of electric vehicle based on cornering stiffness estimation*, in Proc. of IEEE IECON(2005).
- [10] H. Zhou et.al., *Vehicle yaw stability-control system design based on sliding mode and backstepping control approach*, IEEE Trans. Veh. Technol., vol. 59, no. 7(2010), 3674–3678.
- [11] M. Canale et.al., *Vehicle yaw control via second-order sliding mode control*, IEEE Trans. Ind. Electron., vol. 55, no. 11(2008), 3908–3916.
- [12] K. Nam et.al., *Vehicle state estimation for advanced vehicle motion control using novel lateral tire force sensors*, in American Control Conf., Sanfrancisco(2011), 4853–4858.
- [13] K. Nam et.al., *Steering angle-disturbance observer(SA-DOB) based yaw stability control for electric vehicles with in-wheel motors*, in Proc. of Int. Conf. on Control Automation and Systems(2010), 1303–1307.
- [14] H. Sado et.al., *Road condition estimation for traction control in electric vehicle*, in Proc. IEEE Int. Symp. Ind. Electron.(1999), 973–978.
- [15] J.J.E. Slotine and W. Li, *Applied Nonlinear Control*. Englewood Cliffs, NJ: Prentice-Hall, 1991.

## Authors

Mr. Kanghyun Nam received the B.S. degree in mechanical engineering from Kyungpook National University, Daegu, Korea, in 2007 and the M.S. degree in mechanical engineering from Korea Advanced Institute of Science and Technology (KAIST), Daejeon, Korea, in 2009. He is currently working toward the Ph.D. degree in electrical engineering with The University of Tokyo. His research interests include vehicle dynamics and control, state estimation and motion control for electric vehicles, and robust control.



Dr. Sehoon Oh received the B.S., M.S., and Ph.D. degrees in electrical engineering from The University of Tokyo, Tokyo, Japan, in 1998, 2000, and 2005, respectively. He is currently a project research professor in the Department of Electrical Engineering, The University of Tokyo. His research fields include the development of human friendly motion control algorithms and assistive devices for people.



Dr. Hiroshi Fujimoto received the Ph.D. degree in the Department of Electrical Engineering from the University of Tokyo in 2001. In 2001, he joined the Department of Electrical Engineering, Nagaoka University of Technology, Niigata, Japan, as a research associate. From 2002 to 2003, he was a visiting scholar in the School of Mechanical Engineering, Purdue University, U.S.A. In 2004, he joined the Department of Electrical and Computer Engineering, Yokohama National University, Yokohama, Japan, as a lecturer and he became an associate professor in 2005. He is currently an associate professor of the University of Tokyo since 2010. His interests are in control engineering, motion control, nano-scale servo systems, electric vehicle control, and motor drive.



Dr. Yoichi Horii received received B.S., M.S., and Ph.D. degrees in Electrical Engineering from the University of Tokyo, Tokyo, Japan, in 1978, 1980, and 1983, respectively. In 1983, he joined the Department of Electrical Engineering, The University of Tokyo, as a Research Associate. He later became an Assistant Professor, an Associate Professor, and, in 2000, a Professor at the same university. In 2002, he moved to the Institute of Industrial Science as a Professor in the Information and System Division, and in 2008, to the Department of Advanced Energy, Graduate School of Frontier Sciences, the University of Tokyo. From 1991-1992, he was a Visiting Researcher at the University of California at Berkeley. His research fields are control theory and its industrial applications to motion control, mechatronics, robotics, electric vehicles, etc.

Prof. Horii is an IEEE Fellow and an AdCom member of IES. He is a member of the Society of Instrument and Control Engineers; Robotics Society of Japan; Japan Society of Mechanical Engineers; and the Society of Automotive Engineers of Japan. He is the President of Capacitors Forum, and the Chairman of Motor Technology Symposium of Japan Management Association (JMA) and the Director on Technological Development of SAE-Japan (JSAE).

